environments

Article

Evaluation of Operating Parameters for Real Landfill Leachate Treatment via Electrocoagulation

Joana Duarte [1], Diogo Correia [2], João Gomes [1,*] and Eva Domingues [1,*]

[1] CERES, Chemical Engineering and Renewable Resources for Sustainability, Department of Chemical Engineering, Faculty of Sciences and Technology, University of Coimbra, Rua Silvio Lima, 3030-790 Coimbra, Portugal; joana.margarida.duarte@gmail.com
[2] CFE, Centre for Functional Ecology: Science for People & Planet, Department of Life Sciences, University of Coimbra, Calçada Martim de Freitas, 3030-456 Coimbra, Portugal; dcorreia@uc.pt
* Correspondence: jgomes@eq.uc.pt (J.G.); evadomingues@eq.uc.pt (E.D.)

Abstract

Landfill leachate (LL) is a complex wastewater characterized by high concentrations of organic matter and heavy metals, posing significant challenges to conventional treatment technologies. Electrochemical methods, particularly electrocoagulation (ECG), have shown promise for LL treatment; however, issues related to operational optimization and electrode durability remain insufficiently addressed. In this study, a novel electrocoagulation-based approach is proposed that systematically integrates process optimization with an explicit assessment of iron electrode reusability, which is an aspect that has been rarely explored in previous ECG studies on LL. Key operational parameters—current density, pH, inter-electrode distance, electrode surface area, and electrode material—were optimized to enhance treatment performance. Optimal conditions were achieved using iron electrodes at a current density of 256 A/m^2, pH 8, an inter-electrode distance of 1 cm, and an effective electrode surface area of 19.5 cm^2/L. Under these conditions, removal efficiencies of 100% for zinc, 94.9% for copper, and 54.5% for total organic carbon (TOC) were obtained, demonstrating effective simultaneous removal of inorganic and organic contaminants. The electrode reusability tests showed stable removal efficiencies over ten consecutive operational cycles, highlighting the potential for reduced operational costs and improved process sustainability. Additionally, the treated effluent exhibited reduced phytotoxicity, as evidenced by lower germination inhibition (GI), reduced root growth inhibition (RGI), and enhanced removal of humic substances. Overall, the results demonstrate that the proposed ECG approach is a robust, flexible, and environmentally sustainable solution for LL treatment, with clear advantages over conventional EC systems in terms of long-term performance and resource efficiency.

Keywords: humic acid; metal removal; toxicity; electrode; sustainability

Academic Editors: Athanasia K. Tolkou and George Z. Kyzas

Received: 27 November 2025
Revised: 16 January 2026
Accepted: 17 January 2026
Published: 21 January 2026

1. Introduction

Landfill leachate (LL) is a highly contaminated liquid generated by the percolation of water through solid waste in landfills. When inadequately managed, LL can migrate into surrounding soil and water bodies, posing serious risks to environmental and human health. It typically contains a complex mixture of organic and inorganic pollutants, including heavy metals, ammoniacal nitrogen, and emerging contaminants such as pharmaceuticals, plasticisers, and per- and polyfluoroalkyl substances (PFAS) [1,2]. This chemical complexity,

combined with variable pollutant loads, makes LL one of the most challenging waste streams to treat.

Despite European legislation reducing the disposal of biodegradable waste in landfills and introducing measures to control leachate generation, LL continues to represent a major environmental concern. The limited systematic monitoring of LL composition, coupled with the technical and logistical challenges of collection, transport, and treatment, restricts the ability of many conventional wastewater treatment plants (WWTPs) to adequately manage this effluent. While source reduction and waste minimization remain essential for long-term sustainability, effective and scalable treatment technologies are still needed for the LL currently generated.

Recent advances in wastewater treatment technologies—including granular sludge systems, shortcut nitrogen removal pathways, membrane-based processes, and enhanced aeration and control systems—have improved treatment efficiency and energy performance [3]. In parallel, novel treatment strategies extending beyond conventional unit operations have been explored, such as engineered filtration systems using low-cost materials (e.g., sand and industrial ash), which have demonstrated effective removal of organic and inorganic pollutants while offering cost-effective and decentralized treatment solutions [4]. These developments highlight the growing emphasis on sustainable, adaptable, and resource-efficient technologies. Nevertheless, the simultaneous removal of refractory organic compounds, heavy metals, and ammoniacal nitrogen remains technically demanding and often requires integrated or combined treatment approaches [5].

Electrochemical treatment methods have gained attention due to their operational simplicity, relatively low sludge production, short treatment times, and high removal efficiencies [6–8]. These methods have proven effective in removing chemical oxygen demand (COD), ammonia nitrogen, color, and heavy metals from LL [9].

ECG is based on the electrolysis principle in which electricity decomposes compounds. In this process, an electric current is applied between the anode and the cathode, which are submerged in the effluent that intends to be treated. Electrons flow from the anode to the cathode, leading to the corrosion of the anode through oxidation and cathode passivation.

In the initial phase of the electrocoagulation process, metal cations are generated in the anode due to oxidation (Equation (1)). In the cathode, the water reduction reaction leads to the production of hydrogen and hydroxide ions (OH^-) (Equation (2)). While the water reduction reaction occurs on the cathode, at the anode, a water oxidation reaction occurs, producing hydrogen ions (H^+) and oxygen (O_2) (Equation (3)) [10].

$$Metal\ (s) \rightleftharpoons Metal^{n+}(\mathrm{aq}) + \mathrm{ne}^- \quad (1)$$

$$2H_2\mathrm{O(l)} + 2\mathrm{e}^- \rightleftharpoons \mathrm{H_2(g)} + 2OH^-(aq) \quad (2)$$

$$2H_2\mathrm{O(l)} \rightleftharpoons 4H^+(\mathrm{aq}) + \mathrm{O_2(g)} + 4\mathrm{e}^- \quad (3)$$

The metal cations ($Metal^{n+}$) and the hydroxide ions (OH^-) interact, forming metal hydroxides, which are good adsorbents. The contaminants are then destabilized via interaction with the ions formed through the anode oxidation. This results in the compression of the diffuse double layer around the charged species. This compression reduces the electrostatic repulsion between species with the same charge to the point where the Van der Waals attraction predominates, promoting the aggregation of particles. This neutralization leads to the adsorption of destabilized pollutants on the metal hydroxides' surface, forming flocs. These flocs can be separated from the liquid phase by sedimentation or flotation, as the hydrogen formed at the cathode may cause the flocs to rise [11,12].

In addition to treatment innovation, recent studies have demonstrated the potential of advanced electrical analysis techniques for real-time characterization of water quality

changes during treatment processes [13]. Electrical measurements, such as impedance and conductivity, have been demonstrated to capture subtle physicochemical transformations in complex aqueous matrices, underscoring the importance of integrating electrical monitoring tools with treatment performance assessment [14,15]. When considered alongside emerging low-cost and hybrid treatment solutions, these diagnostic approaches further emphasize the importance of developing electrochemical systems that are not only efficient but also scalable, controllable, and environmentally sustainable. By situating the present work within this broader framework of innovative treatment design and advanced diagnostic methodologies, the originality and added value of systematically optimizing combined operational parameters and evaluating ecotoxicological responses in electrocoagulation become more clearly established.

Despite the growing body of research on ECG for LL treatment, most previous studies have focused on short-term pollutant removal performance, often evaluating individual operational parameters in isolation [13,15]. Limited attention has been given to the combined optimization of key operational variables, the long-term performance and reusability of electrodes, and the potential ecotoxicological implications of the treated effluent. These gaps hinder the practical implementation and scalability of ECG systems for real-world applications.

The main objective of this study is to evaluate and optimize the performance of electrocoagulation for LL treatment while addressing key limitations reported in previous studies. Unlike most existing works, which typically investigate individual operating parameters in isolation, this study systematically examines the combined influence of pH, current density, electrode material, and inter-electrode distance on treatment efficiency, providing a more integrated assessment of process performance. In addition, the environmental relevance of the treated effluent is strengthened by coupling conventional removal metrics with phytotoxicity evaluation using *Lepidium sativum* seed germination, which is an aspect rarely considered in electrocoagulation studies focused on LL treatment. By linking operational optimization with toxicity-based assessment, this work advances current state-of-the-art research and offers new insights into the practical applicability, scalability, and sustainability of electrocoagulation for potential agricultural reuse scenarios.

2. Materials and Methods

2.1. Experimental Set-Up

A schematic representation of the experimental setup is presented in Figure 1, where (1) is the 2 L batch reactor placed on top of a magnetic stirrer (2). The anode and the cathode (3) were connected to the electrical power supply (4) (JOpower ALP-3005E III, Alpha Electtronica, Collecchio, Italy) through electrical cables (5).

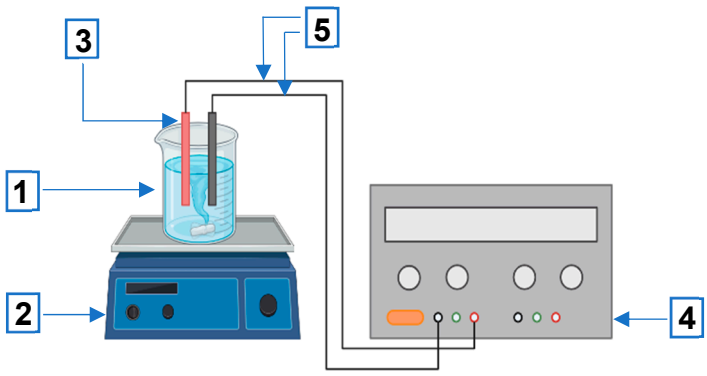

Figure 1. Schematic representation of the experimental set-up.

The electrodes used in this study—iron, stainless steel (SS), and aluminium—had surface areas of 8.6–32.5 cm^2 and were arranged in parallel with interelectrode distances of 1–3 cm. Iron and aluminium are the most widely used sacrificial electrodes in electrocoagulation due to their availability, low cost, and ability to generate effective metal hydroxide coagulants. Aluminium electrodes form Al $(OH)_3$ species with high adsorption capacity but are associated with higher cost and potential residual toxicity, whereas iron electrodes produce Fe^{2+}/Fe^{3+} hydroxides that offer comparable removal efficiency with lower environmental risk and cost [16]. SS was included as a more inert and corrosion-resistant electrode to evaluate electrochemical treatment performance under limited electrode dissolution. The use of these materials enables comparison between conventional sacrificial electrodes and a durable, less reactive alternative, supporting methodological robustness and result transferability [16].

Before each experiment, the anode and cathode were cleaned with 0.1 M HCl and thoroughly rinsed with ultrapure water to remove surface impurities. For the electrode reuse tests, however, no acid cleaning was performed between cycles, ensuring that the reported reusability reflects realistic performance under fouling and passivation conditions rather than chemical regeneration. In each experiment, 1 L of effluent was treated, with a magnetic stirrer speed of 350 rpm to ensure the effluent's homogeneity. After the reaction time, the effluent was left to settle to sediment the flocs that had formed, and the supernatant was collected. In each experiment, the mass loss of the electrodes was determined by weighing them before and after the reaction. Before the final weighing, the electrodes were carefully rinsed and dried, and the mass loss was calculated from the difference between the initial and final masses.

The optimization procedure was conducted sequentially, with each operational parameter optimized individually while keeping the previously optimized parameters constant in subsequent experiments. Initially, the optimal current density was determined using the raw effluent, without any modification other than the addition of the target metals. The optimal conditions identified at each stage were then applied in the subsequent optimization steps. After establishing the overall optimal operating conditions, the kinetic study was performed under these conditions while maintaining isothermal operation. Using the same optimized conditions, electrode reusability experiments were carried out by reusing the same electrodes for ten consecutive cycles to evaluate their stability and performance

2.2. Analytical Techniques

Assessing the physical and chemical properties of an effluent is essential for gaining insight into its potential hazards, identifying the most effective treatment options, and optimizing process conditions. Therefore, parameters such as pH, electrical conductivity (ECD), chemical oxygen demand (COD), total organic carbon (TOC), total solids (TS), total suspended solids (TSS), total dissolved solids (TDS), total Kjeldahl nitrogen (TKN), total nitrogen (TN) and iron, zinc and copper, concentrations, were assessed for the LL studied.

The effluent pH and electrical conductivity were determined using a pH meter (Crison micropH 2002, Barcelona, Spain) and a conductivity meter (Consort C1020, Bruxelles, Belgium), respectively. The COD measurement was performed following the closed reflux colorimetric standard method (5220D) described by Greenberg et al. [17]. A thermoreactor (ECO25—Velp Scientifica, Usmate, Italy) was used for 2 h at 150 °C, followed by a cooling period. A calibration curve using potassium hydrogen phthalate solutions was prepared to determine the COD of the samples. Afterwards, the absorbances were measured in a Multiparameter Photometer (Hanna, HI83399, Nieuwegein, The Netherlands) at 605 nm. The TOC concentration was assessed using a TOC analyzer equipped with an autosampler (ASI-5000A, Shimadzu, Gondomar, Portugal) at the beginning and end of each reaction. The

TS, TSS, and TDS measurements followed the standard method presented by Greenberg et al. [18]. For the TKN measurement, 10 mL of the sample was mixed with a Kjeldahl catalyst tablet and 10 mL of H_2SO_4 (96%). After 2 h of digestion at 400 °C, the mixture was cooled for 1 h, and 100 mL of ultrapure water was added. The solution was then distilled and titrated with HCl (0.1 M) to determine the TKN concentration of the samples. Total Nitrogen (TN) was determined using a TOC analyzer (TOC-5000A, Shimadzu) equipped with an automatic sampler (ASI-5000A, Shimadzu). The sample concentrations of iron, zinc, and copper were determined by flame atomic absorption spectrophotometry (Perkin-Elmer 3300, PerkinElmer U.S. LLC, Shelton, CT, USA). To determine the efficiency of each experiment, the color removal rate was assessed using a T60 UV/VIS (PG Instruments, Ottawa, ON, Canada) spectrophotometer at 400 nm [18].

2.3. ECG Efficiency Evaluation

To evaluate the ECG process efficiency, the removal of TOC and heavy metals was assessed. These removals were determined using Equation (4), where C_0 is the initial pollutant concentration, and C_t is the contaminant concentration at the treatment time t. Color removal was determined by absorbance and calculated using Equation (5), where A_0 is the initial absorbance and A_t is the absorbance at the treatment time t [19].

$$\mathbf{C_{Removal}}(\%) = \frac{\mathbf{C_0 - C_t}}{\mathbf{C_0}} \times \mathbf{100} \tag{4}$$

$$\mathbf{Color_{Removal}}(\%) = \frac{\mathbf{A_0 - A_t}}{\mathbf{A_0}} \times \mathbf{100} \tag{5}$$

Since the electro-based processes require electrical energy, minimizing the energy consumption per gram of TOC removed (EC_{TOC}) is essential. This parameter can be determined by Equation (6) [19].

$$\mathbf{EC_{TOC}}\left(\frac{\mathbf{kWh}}{\mathbf{kg_{TOC}}}\right) = \frac{\mathbf{E_{cell}} \times \mathbf{I} \times \mathbf{t}}{\mathbf{\Delta(TOC)} \times \mathbf{V}} \tag{6}$$

where the energy consumption per mass of TOC units is kWh/kg_{TOC}, the E_{cell} represents the cell's average potential difference (V), the I refers to the current intensity (A), the t is the process time (h), the Δ(TOC) is the TOC removed (gC/L), and the V is the solution volume (L). The determination of energy per solution volume (kWh/m^3) was made through the quotient between energy consumed in the electrocoagulation process and the solution volume used, which was 1 L in all experiments.

Applying current to the electrocoagulation cell leads to the anode dissolution. The mass (m) of the anode that is dissolved was determined based on Faraday's law, Equation (7).

$$\mathbf{m(g)} = \frac{\mathbf{I} \times \mathbf{t} \times \mathbf{M}}{\mathbf{Z} \times \mathbf{F}} \tag{7}$$

where m is the mass of the anode dissolved (g), I is the current intensity (A), t is the time of electrocoagulation (s), M is the molar mass of the electrode material used (g/mol), Z is the valence electrons of the metal, and F is Faraday's constant (96,485 C/mol). The reaction kinetics were assessed by plotting the removal rates in order of energy, as determined by Equation (8).

$$\mathbf{Energy(Wh)} = \mathbf{P} \times \mathbf{t} = \mathbf{I} \times \mathbf{E_{cell}} \times \mathbf{t} \tag{8}$$

The integral method was used to determine the reaction order, the rate constant, and each contaminant's half-life. Three plots were made: contaminants' concentrations versus time (zeroth-order reaction), the natural logarithm of concentration versus time (first-order

reaction), and the inverse of the concentration versus time (second-order reaction). The graph with the highest coefficient of determination (R^2) value determined the order of the reaction. Once the reaction order was determined, the rate constant (k) and the half-life for each pollutant were assessed. Table 1 presents the equations necessary to determine the half-life of each pollutant according to the reaction order, where C_0 represents the contaminant concentration at the beginning of the reaction, and k represents the rate constant.

Table 1. Equations to determine the half-life according to the reaction order.

Reaction Order	Half-Life
0	$\frac{C_0}{2k}$
1	$\frac{\ln(2)}{k}$
2	$\frac{1}{kC_0}$

2.4. Ecotoxicity Evaluation

Phytotoxicity tests were conducted on *Lepidium sativum* following ISO 18763 [20]. Artificial soil (85% fine dry sand, 10% kaolinite clay, 5% peat) was mixed with 30 mL of either the sample or ultrapure water (control), with the pH pre-adjusted to 7.12 ± 0.14. Ten seeds were evenly placed on a wet filter paper, and the assay was performed in triplicate. Samples were incubated in the dark at 25 °C for 72 h. Ultrapure water was used as a blank to assess baseline seed growth. After 72 h, seed germination and root length were recorded to evaluate phytotoxic effects. This test determines the germination and root growth inhibition through Equation (9), where $X_{control}$ is the number of germinated seeds or the root length in the control test, and X_{sample} is the number of germinated seeds or the root length in the tested samples.

$$\mathbf{X_{Inhibition}(\%)} = \frac{\mathbf{X_{control} - X_{sample}}}{\mathbf{X_{control}}} \times \mathbf{100} \quad (9)$$

The humic acid removal was determined by UV spectroscopy. A concentrated stock solution was prepared by dissolving 206.8 mg of humic acids in 1 L of a 4 g/L NaOH solution. The stock solution was then diluted to solutions with humic acid concentrations of 5, 10, 20, 30, 35, 40, and 50 mg/L to prepare a calibration curve. It was possible to determine the humic acid concentration in the samples using a T60 UV/VIS (PG Instruments) spectrophotometer at 465 nm, and the calibration curve. The humic acid removal efficiency was determined through Equation (5) [21].

3. Results and Discussion

3.1. Effluent Characterization

The LL used in this study was collected from a landfill site in the Center region of Portugal. LL can be classified as young, intermediate, or old depending on its age. Young leachate corresponds to a landfill age of less than five years and is characterized by high COD and biochemical oxygen demand (BOD) values, and medium concentration of heavy metals. Its organic compounds are mainly volatile fatty acids (VFA). Intermediate leachate (5 to 10 years) has lower COD and BOD values and a low concentration of heavy metals. These leachate organic compounds are mainly humic and fulvic acids, and are characterized by being persistent and recalcitrant, with some VFA. Old leachate, with a landfill age exceeding ten years, exhibits low COD and BOD values, resulting in reduced biodegradability. Heavy metal concentration is also low, and the organic compounds are humic and fulvic acids [22].

To simulate the concentration of heavy metals in an intermediate leachate, as presented by Gómez et al. [22], approximately 25 mg of copper (II) nitrate trihydrate ($CuN_2O_6 \cdot 3H_2O$), 65 mg of ferrous sulfate heptahydrate ($FeSO_4 \cdot 7H_2O$), and 27 mg of zinc oxide (ZnO) were added to the effluent. After adding the metals, the effluent was stirred for 30 min to ensure its homogeneity, and an initial sample was taken. Table 2 presents the leachate's most important physical and chemical properties: pH, COD, TOC, TS, TSS, TDS, electrical conductivity (ECD), TKN, TN, and iron, zinc, and copper concentrations.

Table 2. Landfill leachate's physical and chemical properties.

Property	Units	Value
pH	-	8.10 ± 0.05
COD	mg/L	3110.7 ± 163.0
TOC	mg/L	531.1 ± 16.9
TS	g/L	13.72 ± 0.70
TSS	g/L	0.12 ± 0.02
TDS	g/L	13.07 ± 0.10
ECD	mS/cm	11.1 ± 0.30
TKN	mg/L	71.2 ± 11.6
TN	mg/L	255.0 ± 18.9
Iron	mg/L	10.65 ± 3.60
Zinc	mg/L	6.12 ± 1.60
Copper	mg/L	11.28 ± 1.40

The values obtained for the physical and chemical properties of the used leachate were compared to those presented by Gómez et al. [22]. It was possible to conclude that the characteristics of the used leachate correspond to those of an intermediate leachate, mainly due to its COD value.

3.2. Electrocoagulation: Parameters Optimization

3.2.1. Effect of Current Density

Several operating parameters influence the efficiency of the electrocoagulation process. Therefore, optimizing landfill leachate treatment using electrocoagulation involved studying the impact of different variables on zinc, iron, copper, TOC, and color removals.

Firstly, the effect of current density was evaluated using iron electrodes at the raw leachate pH. A previous study showed that increasing the current density from 256 to 513 and 1026 A/m^2 had minimal influence on COD and heavy metals removal. However, this increase in current density could be insufficient to achieve higher process efficiencies. The effect of current densities of 256 and 2051 A/m^2 was compared, as presented in Figure 2a. By analysing Figure 2a, it can be concluded that increasing the current density from 256 to 2051 A/m^2 led to a significant increase in the zinc (from 45.9% to 82.3%), iron (from 41.1% to 99.9%), and color (from 58.8% to 80.9%) removals. Additionally, there is an increase in TOC removal, from 31.9% to 42.1%. These results were expected since the current density determines the amount of Fe^{2+} ions released from the anode, which are responsible for coagulant production. As such, higher current densities lead to greater anode dissolution and, consequently, higher Fe $(OH)_3$ floc production, promoting pollutant removal. Furthermore, increasing the current density promotes the production of hydrogen bubbles, which leads to greater pollutant removal through flotation [23].

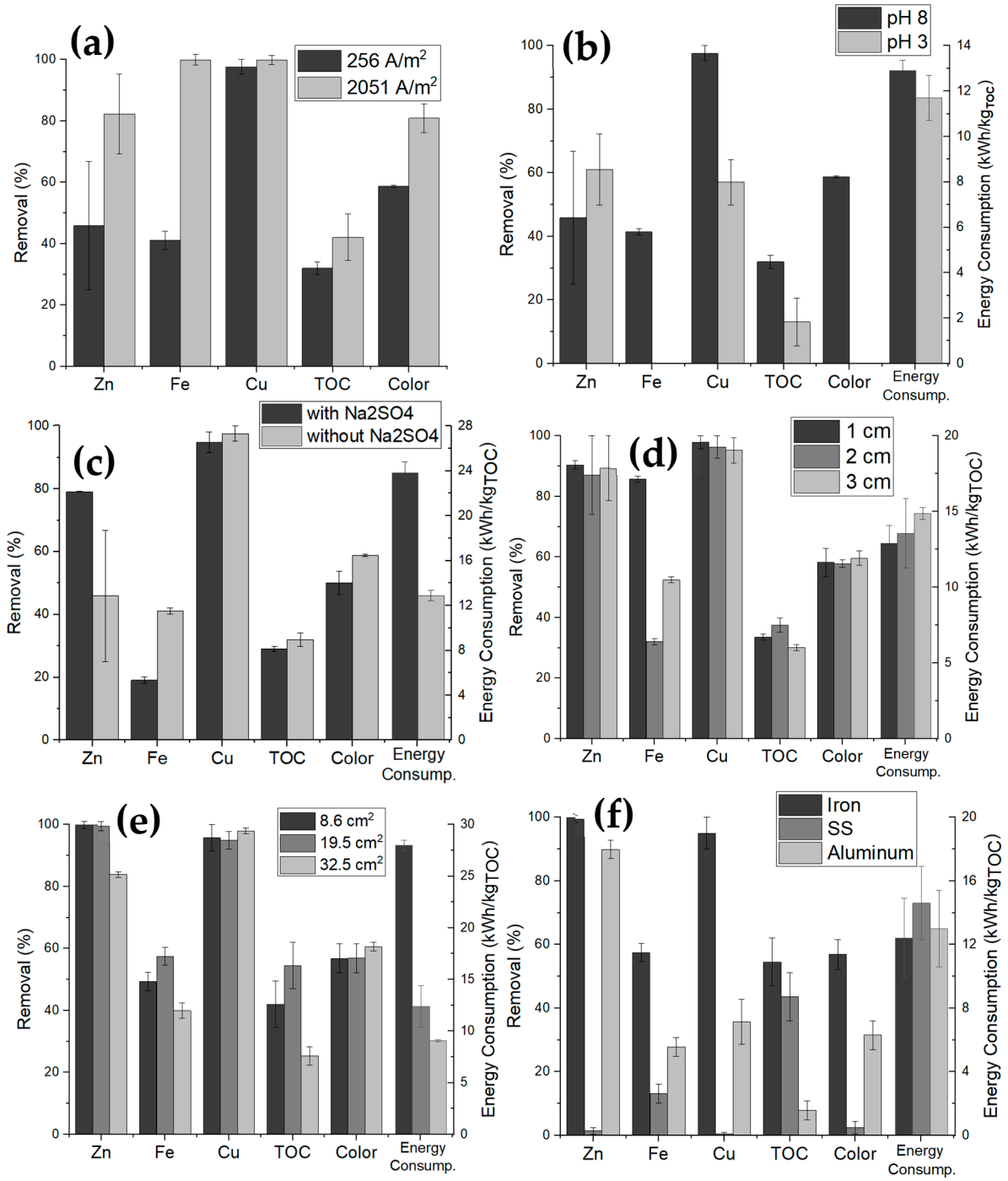

Figure 2. Removal rates and energy consumption obtained by electrocoagulation for the optimization of (**a**) current density, (**b**) pH, (**c**) electrolyte, (**d**) distance between electrodes, (**e**) electrode effective surface area, (**f**) electrode material.

However, higher current densities mean higher energy consumption, which is an operational energetic waste that is noticeable through a temperature rise in the solution. Additionally, higher current densities will enable secondary reactions, with operational life of the electrodes being reduced and the presence of electrode material at the solution. To further understand the influence of the current density, the energy consumption (EC) was determined through Equation (6), the theoretical anode mass loss through Equation (7), and the experimental anode mass loss, and the highest temperature rise was recorded. Table 3 presents the values of the parameters previously named for each current density (256 and

2051 A/m^2). The results presented in Table 3 show that the energy consumption when applying a current density of 2051 A/m^2 is almost 24 times higher than when applying 256 A/m^2. Based on that, we conclude that there is an energy waste when conducting electrocoagulation at 2051 A/m^2, shown by a temperature increase to 52 °C, contrasting with no temperature rise when applying a current density of 256 A/m^2. Faraday's law proved to be efficient in determining the anode mass dissolved for each current density. The anode mass loss for the highest current density was approximately eight times higher than that for 256 A/m^2. Therefore, the lowest current density (256 A/m^2) was chosen for the experiments to follow since it exhibits good performance, no energy waste, and a lower anode mass loss, which decreases the cost of the process.

Table 3. Energy consumption (EC), theoretical and experimental mass loss, and temperature rise for electrocoagulation at 256 and 2051 A/m^2.

Current Density (A/m^2)	EC (kWh/kg$_{TOC}$)	Theoretical Mass Loss (g)	Experimental Mass Lost (g)	Temperature Rise (°C)
256	12.9	0.52	0.52	-
2051	307.4	4.18	4.15	52

3.2.2. pH Effect

The influence of pH on ECG efficiency was evaluated using iron electrodes at the raw leachate pH (8.0) and at pH 3.0. The effluent pH was adjusted at the beginning of the experiment using a 1 M H_2SO_4 solution, with no further pH correction during the reaction. Figure 2b shows the removal efficiencies at the two pH values tested in the work. Electrocoagulation at pH 8.0 achieved iron, copper, TOC, and color removal rates that were 41.1, 40.6, 18.9, and 58.8 percentage points higher, respectively, than those obtained at pH 3.0. This difference can be attributed to the effect of pH on coagulant speciation, as indicated by the iron Pourbaix diagram [24]. At pH 8, Fe $(OH)_3$ flocs dominate, providing effective adsorption sites for contaminants. In contrast, at pH 3.0, soluble Fe^{2+} is the predominant species, and Fe $(OH)_3$ formation is limited, reducing removal efficiency. Furthermore, the lower pH can promote the generation of hydroxyl radicals via the electro-Fenton process due to the presence of transition metals in the leachate, offering an additional degradation pathway. However, the dominant removal mechanism under these conditions remains limited by the low floc formation. Additionally, operating at pH 3.0 requires chemical addition for adjustment, which increases treatment costs, making neutral to slightly alkaline conditions more practical for landfill leachate electrocoagulation. The energy consumption for electrocoagulation at pH 8.0 and 3.0 was 12.9 and 11.7 kWh/kg$_{TOC}$, respectively. No significant difference in energy consumption is verified because the leachate's conductivity remained unchanged despite the pH adjustment. Similar findings were reported by Asaithambi et al. [25]. Since electrocoagulation exhibits better removal efficiencies at pH 8.0, the following optimizations were performed at this pH.

3.2.3. Effect of Electrolyte Addition

To assess the effect of solution conductivity, 5 g of Na_2SO_4 were added as a supporting electrolyte. Beyond increasing conductivity, Na_2SO_4 can participate in electrochemical reactions, generating sulfate radicals that may enhance contaminant degradation, highlighting its mechanistic role in the process [26]. This way, the electrical conductivity of the leachate increased from 11.1 to 15.6 mS/cm. By adding an electrolyte to the effluent, the process efficiency is expected to be enhanced. This is due to increased electrical conductivity that reduces the total resistance, resulting in higher ion mobility and reduced energy

consumption. Analysis of Figure 2c indicates that the addition of Na_2SO_4 did not enhance process efficiency as anticipated and instead resulted in increased energy consumption, with comparable findings reported by Turro et al. [27]. These results can be explained through the enhancement of oxygen evolution by Na_2SO_4, which is a side reaction that can limit the electro-generation of oxidants, such as chlorine/hypochlorite, which are produced when chlorine is present in the effluent. On the other hand, Keyikoglu et al. [28] stated that the decrease in process efficiency could be due to the reaction between SO_4^{2-} ions and iron hydroxides. This reaction decreases the amount of iron hydroxides in the solution, which are responsible for the coagulation of pollutants, leading to a decrease in pollutant removal. The increase in energy consumption (from 12.9 to 23.8 kWh/kg_{TOC}) can be explained by the energy expended on the side reactions instead of in direct pollutant removal. Since the addition of Na_2SO_4 did not improve the removal efficiencies, the subsequent reactions were performed without adding this compound for cost minimization.

3.2.4. Effect of Electrode Distance

The distance between electrodes influences the system's electrostatic field and, subsequently, the movement of ions. Three inter-electrode distances (1, 2, and 3 cm) were tested using iron electrodes for 1 h. Figure 2d presents the removal rates obtained for the different distances between the iron electrodes. An optimal inter-electrode distance results in a slower ion movement, enhancing floc production and increasing pollutant removal rates. From analysing Figure 2d it is observed that increasing the inter-electrode distance from 1 to 3 cm leads to a slight decrease in the removal rates. This can be explained since higher inter-electrode distances represent longer distances that the ions must travel, reducing the electrostatic attraction and decreasing the quantity of flocs produced for coagulation. On the other hand, lower inter-electrode distances minimize the solution's resistance, requiring less energy to move ions due to their shorter travel distance. As such, energy consumption decreases as the inter-electrode distance is reduced (14.9 kWh/kg_{TOC} at 3 cm to 12.9 kWh/kg_{TOC} at 1 cm), as shown in Figure 2d. Beiramzadeh et al. [29] reported similar findings since increasing the inter-electrode distance from 1 to 2.5 cm decreased nickel and iron removal efficiency from 94% to 84.5% and 93.3% to 80%, respectively. The inter-electrode distance of 1 cm was chosen as optimal and used for the following experiments due to its good performance and lower energy consumption.

3.2.5. Effect of the Electrode's Effective Surface Area

The effective surface area of the electrode plays a crucial role in electrocoagulation performance, as it directly influences the rate of anode dissolution and the generation of Fe^{2+} ions. To assess this effect, electrocoagulation experiments were carried out using iron electrodes with surface areas of 8.6, 19.5, and 32.5 cm^2. The electrodes had a width and a length of 2.5 × 1.7, 2.5 × 3.9 and 2.5 × 6.5, respectively. The effective electrode area was calculated by multiplying the width and the length by two, considering that each electrode has two active sides. In principle, an increase in electrode surface area is expected to enhance pollutant removal due to the higher production of Fe^{2+} ions and, consequently, a greater availability of coagulant species. However, as shown in Figure 2e, the largest electrode area (32.5 cm^2) did not result in the highest pollutant removal efficiency, contrary to this expectation.

This apparent contradiction can be explained by the fact that the coagulant dose generated with an electrode surface area of 19.5 cm^2 was already sufficient to destabilize and remove the pollutants present in the leachate. Further increases in surface area likely led to excessive formation of iron hydroxide flocs, which can hinder mass transfer by increasing solution turbidity and limiting effective contact between pollutants and reactive

species. In addition, the overproduction of Fe^{2+} ions may promote parasitic side reactions, such as unnecessary iron oxidation and oxygen evolution, which do not contribute to pollutant removal and may reduce overall process efficiency.

Despite the lack of improvement in removal performance, increasing the electrode surface area resulted in a significant reduction in energy consumption. As illustrated in Figure 2e, energy demand decreased from 28.1 to 12.4 and 9.1 kWh/kg_{TOC} when the electrode area increased from 8.6 to 19.5 and 32.5 cm^2, respectively. This reduction can be attributed to the lower current density per unit area and reduced cell voltage associated with larger electrodes, which decrease electrical resistance and energy losses. Therefore, while larger electrode areas improve energy efficiency, they do not necessarily enhance pollutant removal due to limitations imposed by excessive floc formation, mass-transfer constraints, and parasitic electrochemical reactions. Angarnokolaei et al. [30] obtained similar results, which are explained by the fact that higher electrode areas reduce the electrical resistance, decreasing the voltage required to obtain a constant electric current. Considering these results, the optimal electrode effective surface area chosen was 19.5 cm^2.

The electrocoagulation reaction mechanism depends on several factors, including pH, current density, electrolyte composition, wastewater characteristics, and also the electrode material, as illustrated in Table 1. Therefore, the process efficiency using iron, stainless steel (SS), and aluminium electrodes was compared. Analysis of Figure 2f reveals that iron electrodes achieve the highest removal rates. On the other hand, the efficiency of electrocoagulation using aluminium and SS electrodes was lower. This could be explained by the fact that the ferric hydroxides could have a higher adsorption capacity than those of aluminium and SS. Concerning the results obtained using SS electrodes, it was observed that this material led to low removal efficiencies for zinc, iron, and copper (1.4%, 13.1%, and 0.5%, respectively), while achieving a notable TOC removal of 43.6%. This could be attributed to the possible indirect oxidation of organic matter in the solution via electro-generated hydroxyl radicals. Additionally, the lower values for heavy metals removal can be explained by the fact that SS is prone to passivation, inhibiting the dissolution of the electrode. Although the energy consumption values are similar across all materials, iron exhibits the lowest consumption, followed by aluminium, while SS shows the highest. These differences can be attributed to the electrical conductivity, overpotential, and passivation characteristics of each material [31]. Based on its high removal efficiency and lower energy consumption, iron was selected for use in the subsequent experiments.

3.2.6. Reusability Tests

One of the main disadvantages of electrocoagulation is the need for constant electrode replacement due to anode dissolution and cathode passivation. Therefore, it is crucial to evaluate the reusability of the electrodes to promote environmental sustainability. Electrocoagulation was performed ten times with the same iron electrodes at the previously determined optimal conditions. The results obtained are presented in Table 4. Iron, copper, and zinc removal efficiencies did not decrease significantly from the first reuse to the tenth. Some variations on the metals analysed can be found along the cycles, which can be related to the inherent variability of the analytical technique considered. These results demonstrate that, despite anode dissolution and the formation of a passive layer on the cathode, the same electrodes can be reused at least ten times without significant changes in process efficiency. The theoretical anode mass loss determined by Faraday's law was 5.73 g, and the experimental mass loss registered was 5.68 g. These findings indicate that anode mass loss remains consistent across reutilizations. This is a promising outcome, as electrode reuse can reduce process costs and enable the treatment of larger effluent volumes with lower iron consumption.

Table 4. Average values (±standard deviation) of removal efficiency (%) during electrode reutilization cycles.

Reutilization Cycle	Zinc (%)	Iron (%)	Copper (%)
0	87.1 ± 2.4	46.3 ± 2.1	96.9 ± 1.2
1	100.0 ± 2.0	60.0 ± 2.5	96.5 ± 1.0
2	92.2 ± 1.8	76.5 ± 2.8	97.1 ± 1.1
3	87.1 ± 2.2	39.7 ± 2.6	97.0 ± 1.0
4	87.1 ± 2.1	44.2 ± 2.4	96.6 ± 1.2
5	87.5 ± 2.0	47.3 ± 2.5	97.7 ± 1.1
6	100.0 ± 1.9	64.0 ± 2.7	96.8 ± 1.0
7	100.0 ± 1.7	52.8 ± 2.9	97.0 ± 1.1
8	100.0 ± 1.6	84.0 ± 3.0	97.8 ± 1.0
9	96.7 ± 2.0	31.2 ± 2.8	93.5 ± 1.3
10	81.2 ± 2.3	52.5 ± 2.6	100.0 ± 1.1

3.2.7. Kinetics Analysis

Under the optimal operating conditions (current density of 256 A/m^2, pH 8.0, inter-electrode distance of 1 cm, effective electrode surface area of 19.5 cm^2, and iron electrodes), removal efficiencies of 100% for zinc, 57.5% for iron, 94.9% for copper, 54.5% for TOC) and 56.9% for color were achieved. Although the TOC removal was moderate compared to that of heavy metals, a reduction of approximately 54% represents a substantial decrease in the organic load of LL. Such a reduction can significantly improve effluent biodegradability and lower the burden on downstream treatment units in wastewater treatment plants, facilitating compliance with typical discharge limits when electrocoagulation is applied as a pre-treatment step. Moreover, this level of TOC removal contributes to improved effluent quality for potential non-potable reuse scenarios, where partial organic matter removal is often sufficient before polishing treatments. The treatment kinetics under these conditions were subsequently evaluated in relation to energy consumption, as described by Equation (8). The kinetics were performed assuming isothermal conditions (T = 25 °C) since by using a current density of 256 A/m^2, there is no Joule heating, as can be seen in Table 3. Furthermore, the solution temperature was continuously monitored throughout each kinetic run to ensure that no significant temperature variation occurred during the experiments. Figure 3 illustrates the removal rates of heavy metals, TOC, and color over 120 min.

Analysing Figure 3 reveals that the pollutant removal rates over time show similar behaviour, except for iron. The iron removal rate is −84.7% at 10 min (0.23 Wh), then increases and exhibits a growth similar to the other pollutants. This decrease in iron removal until the tenth minute occurs due to anode dissolution, which results in a higher iron concentration in the solution. Over time, the iron in the solution forms coagulants or is adsorbed by them, decreasing its concentration in the leachate and increasing the iron removal rate. The results in Figure 3 also indicate that zinc and copper were completely removed at energy consumptions of 0.35 Wh and 2.1 Wh, corresponding to 15 and 90 min, respectively. The highest copper, TOC, and color removal rates are achieved at 90, 120, and 120 min, respectively (2.1 and 2.8 Wh). However, the difference between the removal rates achieved at 60 min (1.4 Wh) and those achieved at 90 and 120 min is only around 3%, 6%, and 4% for copper, TOC, and color, respectively. Hence, electrocoagulation can be performed for 60 min (1.4 Wh) since, at this time, zinc has been completely removed, iron achieves its highest removal rate, and there is no significant increase in the removal rates of copper, TOC, and color with longer electrocoagulation times. The reaction order, rate constant (k), and half-life were determined for the removal of each pollutant. Table 5 summarizes these kinetic parameters for zinc, iron, copper, TOC, and color.

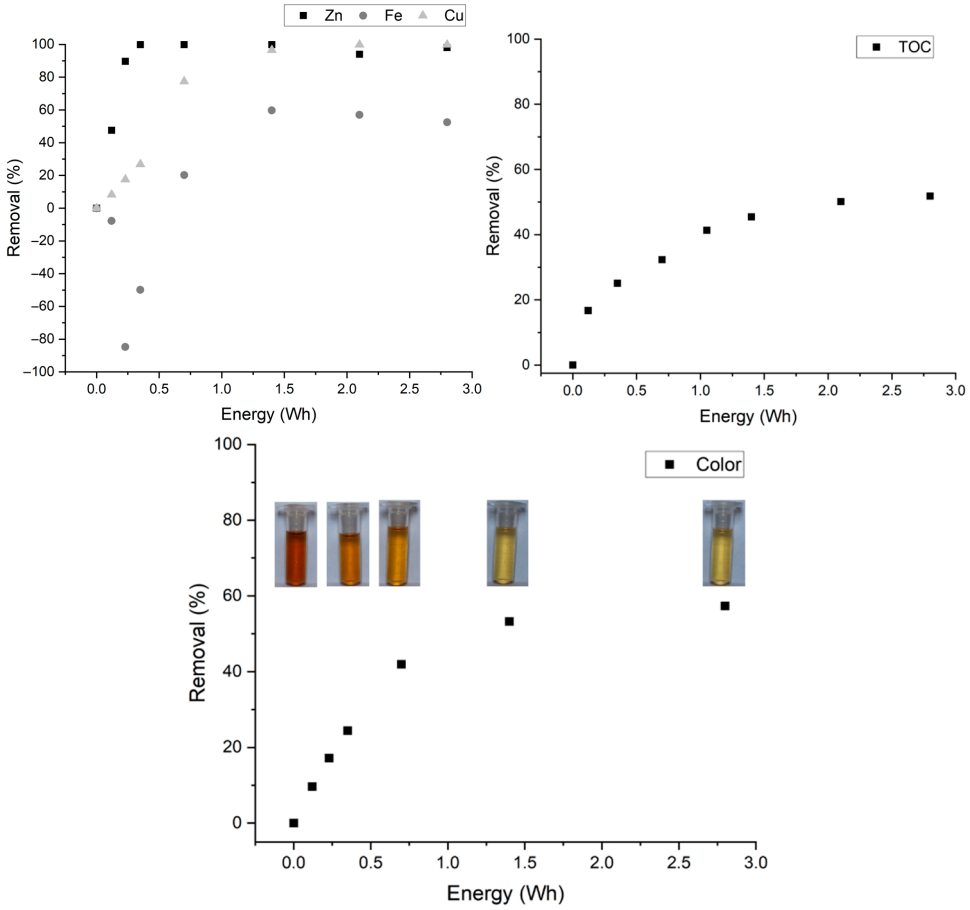

Figure 3. Removal rates of heavy metals, TOC, and color were obtained by performing electrocoagulation under the optimized conditions over 120 min (standard error was <5%).

Table 5. Reaction order, coefficient of determination (R^2), rate constant (k), and half-life were determined for each pollutant for electrocoagulation.

Pollutant	Reaction Order	R^2	k	Half-Life (min)
Zinc	0	0.999	0.049 (mg/L·min)	5.6
Iron	1	0.878	0.037 (1/min)	18.8
Copper	1	0.978	0.059 (1/min)	11.1
TOC	2	0.988	6×10^{-6} (L/mg·min)	254.1
Color	2	0.982	0.004 (1/min)	51.3

Analysis of Table 5 reveals that the removal of heavy metals followed zeroth- and first-order kinetics, whereas the removal of TOC and color adhered to second-order kinetics. Iron shows a low coefficient of determination (R^2), interpreted as a poor fit to the reaction order. The electrocoagulation process is more efficient at removing heavy metals than organic matter, as evidenced by the lower half-life values for heavy metals compared to those for TOC and color. Since the landfill leachate color is mainly due to the humic acid in the solution, and since these compounds represent most of the organic compounds present in landfill, color removal is also characterized by higher half-life values and lower rate constant values than heavy metals.

3.2.8. Ecotoxicity Tests

To evaluate the efficiency of the process and assess the environmental impact of treated leachate, phytotoxicity tests were conducted. The pH used in this evaluation was pre-adjusted to 7.12 ± 0.14 and the characterization of effluent regarding TOC and residual dissolved metals composition was 164.9 mgC/L, 0.33 mgIron/L, and 0.27 mgCopper/L for the treated effluent and 362.5 mgC/L, 7.2 mgIron/L, 5.1 mgZinc/L, and 10.3 mgCopper/L for the landfill leachate. Furthermore, humic acid removal efficiency was also evaluated through UV spectroscopy. Humic acids present in landfill leachate pose considerable challenges due to their low biodegradability, high chemical oxygen demand (COD), and their influence on the mobility of metals and metalloids. These complex organic molecules are largely responsible for the brown coloration of leachate, impairing biological treatment efficiency and disrupting metal recovery or extraction processes [32,33]. These tests were conducted on leachate obtained by performing ECG at the optimized conditions. Table 6 presents the results obtained by the phytotoxicity test regarding germination inhibition (GI) and root growth inhibition (RGI), and the standard error of these measures. The humic acid removal (HAR) results obtained by UV spectroscopy are also shown in Table 6 for the optimized processes. The electrocoagulation treatment allows for achieving higher removals of toxic organic compounds and heavy metals. As such, lower GI and RGI values and higher removals of humic acid were achieved in the processes when ECG was applied.

Table 6. Germination inhibition (GI), root growth inhibition (RGI) and humic acid removal (HAR) were obtained for the processes with the best performance.

Process	GI (%)	RGI (%)	HAR (%)
Landfill leachate	50.0 ± 17.3	78.1 ± 5.8	-
ECG	26.7 ± 5.4	57.2 ± 15.5	12.5

The application of ECG in treatment LL has demonstrated several significant benefits, particularly in terms of improving the environmental quality and safety of the treated effluents or materials. One of the most notable advantages observed was the reduction in Germination Inhibition (GI) and Root Growth Inhibition (RGI) values. These parameters are widely used as indicators of phytotoxicity and ecological impact. Lower GI and RGI values suggest that the treated samples exhibited reduced levels of toxicity, thereby promoting better seed germination and healthier root development in bioassays. This improvement indicates that ECG treatment outputs may be more suitable for agricultural reuse or safe environmental discharge, aligning with sustainable waste management and resource recovery practices.

The electrocoagulation performance obtained in this study was compared with that reported by Asaithambi et al. [25]. In the referenced study, maximum removal efficiencies of 74.57% for color and 51.75% for TOC were achieved at a current density of 5.25 A/dm^2, pH 7.83, and an inter-electrode distance of 1 cm, with an associated energy consumption of 14.80 kWh/m^3. Under ideal conditions and comparable pH and inter-electrode spacing, the present study achieved a similar TOC removal efficiency (54.5%), although color removal was lower (56.9%).

Despite the slightly lower color removal, the process demonstrated markedly improved energy performance, with an energy consumption of 1.4 kWh/m^3. This enhanced energy efficiency can be attributed to the optimized current density (256 A/m^2) and effective electrode surface area, which promoted efficient pollutant destabilization while minimizing electrical energy demand.

Furthermore, the present study achieved complete zinc removal and high copper removal efficiency (94.9%), highlighting a strong capability for heavy metal removal along-

side organic matter reduction. These results indicate that the material selected as the electrode and the operating conditions employed favour metal precipitation and coagulation mechanisms, while maintaining TOC removal levels comparable to those previously reported [34].

Overall, the comparison indicates that similar organic matter removal can be achieved at substantially lower energy consumption, highlighting the potential of the proposed electrocoagulation configuration as a more energy-efficient alternative for landfill leachate treatment.

4. Conclusions

The ECG process evaluated in this study demonstrates significant potential as an effective and adaptable solution for landfill leachate treatment. By systematically optimizing key operational parameters—including current density, pH, inter-electrode distance, effective electrode surface area, and electrode material—this work identifies conditions that maximize pollutant removal while minimizing energy consumption.

The optimal performance was achieved using iron electrodes at a current density of 256 A/m^2, pH 8.0, an inter-electrode distance of 1 cm, and an effective surface area of 19.5 cm^2/L. Under these conditions, removal efficiencies reached 100% for zinc, 94.9% for copper, and 54.5% for TOC, highlighting the process's strong capability to address both inorganic and organic contaminants.

A key contribution of this study is the demonstration of electrode reusability, one of the main limitations of conventional electrocoagulation systems. Over ten operational cycles, no significant decline was observed for copper, iron, or zinc removal. These results indicate that electrode reuse is feasible, offering clear advantages in terms of cost reduction, lower environmental impact, and improved sustainability of the process.

Despite these positive outcomes, the moderate TOC removal highlights a limitation, suggesting that additional post-treatment (e.g., biological polishing or membrane filtration) may be required to meet stricter water quality or reuse standards. Nevertheless, the observed reduction in phytotoxicity, as evidenced by GI and RGI, along with the removal of humic substances, reinforces the practical applicability of ECG-treated effluent for safer discharge or irrigation purposes.

Looking forward, the scalability of this technology could be further explored through pilot-scale applications, integration with complementary processes such as membrane filtration, or the use of renewable energy sources, such as solar-powered electrocoagulation systems. Such developments could validate performance under real-world conditions and enhance the economic and environmental viability of large-scale ECG operations.

Overall, this study demonstrates that optimized electrocoagulation is a robust, flexible, and environmentally sustainable strategy for landfill leachate treatment, with clear potential for scale-up and cost-effective implementation.

Author Contributions: Conceptualization, E.D. and J.G.; methodology, J.D. and D.C.; validation, D.C., J.G. and E.D.; formal analysis, J.G. and E.D.; investigation, J.D.; resources, J.G. and E.D.; data curation, J.D. and E.D.; writing—original draft preparation, J.D., D.C., J.G. and E.D.; writing—review and editing, D.C., J.G. and E.D.; supervision, E.D.; project administration, E.D.; funding acquisition, J.G. and E.D. All authors have read and agreed to the published version of the manuscript.

Funding: The authors gratefully acknowledge FCT (Fundação para a Ciência e Tecnologia, Portugal) for their financial support (CEECIND/01207/2018) with the identifier https://doi.org/10.54499/CEECIND/01207/2018/CP1585/CT0003. Thanks to FCT/MCTES for the financial support to CERES (UIDB/00102/2025) with the identifiers https://doi.org/10.54499/UID/00102/2025, https://doi.org/10.54499/UID/PRR/00102/2025.

Data Availability Statement: The data presented in this study are available upon request from the corresponding author due to privacy reasons.

Conflicts of Interest: The authors declare no conflicts of interest.

References

1. Koda, E.; Miszkowska, A.; Sieczka, A. Levels of organic pollution indicators in groundwater at the old landfill and waste management site. *Appl. Sci.* **2017**, *7*, 638. [CrossRef]
2. El-Saadony, M.T.; Saad, A.M.; El-Wafai, N.A.; Abou-Aly, H.E.; Salem, H.M.; Soliman, S.M.; El-Mageed, T.A.A.; Elrys, A.S.; Selim, S.; El-Hack, M.E.A.; et al. Hazardous wastes and management strategies of landfill leachates: A comprehensive review. *Environ. Technol. Innov.* **2023**, *31*, 103150. [CrossRef]
3. Wang, J.; Qiao, Z. A comprehensive review of landfill leachate treatment technologies. *Front. Environ. Sci. Sec. Water Wastewater Manag.* **2024**, *12*, 1439128. [CrossRef]
4. El Hafidi, E.M.; Mortadi, A.; Lizoul, B.; Hairch, Y.; Mghaiouini, R.; Sabor, A.; Mnaouer, K.; Chahid, E.G.; Jebbari, S.; El Moznine, R.; et al. Assessment of sand and hearth ash filtration for wastewater treatment and novel monitoring via complex conductivity. *Euro-Mediterr. J. Environ. Integr.* **2025**, *10*, 1137–1148. [CrossRef]
5. Kurniawan, T.A.; Lo, W. Removal of refractory compounds from stabilized landfill leachate using an integrated H2O2 oxidation and granular activated carbon (GAC) adsorption treatment. *Water Res.* **2009**, *43*, 4079–4091. [CrossRef] [PubMed]
6. Zhang, M.; Shi, Q.; Song, X.Z.; Wang, H.; Bian, Z.Y. Recent electrochemical methods in electrochemical degradation of halogenated organics: A review. *Environ. Sci. Pollut. Res.* **2019**, *26*, 10457–10486. [CrossRef]
7. Bakry, S.A.; Matta, M.E.; Zaher, K. Electrocoagulation process performance in removal of TOC, TDS, and turbidity from surface water. *Desalination Water Treat.* **2018**, *129*, 127–138. [CrossRef]
8. Shaker, O.A.; Safwat, S.M.; Matta, M.E. Nickel removal from wastewater using electrocoagulation process with zinc electrodes under various operating conditions: Performance investigation, mechanism exploration, and cost analysis. *Environ. Sci. Pollut. Res.* **2023**, *30*, 26650–26662. [CrossRef]
9. Pirsaheb, M.; Azizi, E.; Almasi, A.; Soltanian, M.; Khosravi, T.; Ghayebzadeh, M.; Sharafi, K. Evaluating the efficiency of electrochemical process in removing COD and NH4-N from landfill leachate. *Treatment* **2016**, *15*, 6644–6651. [CrossRef]
10. Huang, C.H.; Shen, S.Y.; Dong, C.D.; Kumar, M.; Chang, J.H. Removal mechanism and effective current of electrocoagulation for treating wastewater containing Ni (II), Cu (II), and Cr (VI). *Water* **2020**, *12*, 2614. [CrossRef]
11. Ammar, M.; Yousef, E.; Mahmoud, M.A.; Ashraf, S.; Baltrusaitis, J. A Comprehensive Review of the Developments in Electrocoagulation for the Removal of Contaminants from Wastewater. *Separations* **2023**, *10*, 337. [CrossRef]
12. Jovanović, T.; Velinov, N.; Petrović, M.; Najdanović, S.; Bojić, D.; Radović, M.; Bojić, A. Mechanism of the electrocoagulation process and its application for treatment of wastewater: A review. *Adv. Technol.* **2021**, *10*, 63–72. [CrossRef]
13. Guo, Z.; Zhang, Y.; Jia, H.; Guo, J.; Meng, X.; Wang, J. Electrochemical methods for landfill leachate treatment: A review on electrocoagulation and electrooxidation. *Sci. Total Environ.* **2022**, *806*, 150529. [CrossRef]
14. El Hafidi, E.M.; Mortadi, A.; Chahid, E.G.; Laasri, S. Effect of trichloroisocyanuric acid concentration on the electrical properties of swimming pool water. *Sci. Rep.* **2025**, *15*, 5223. [CrossRef] [PubMed]
15. Galvão, N.; Souza, J.B.; Vidal, C.M.S. Landfill leachate treatment by electrocoagulation: Effects of current density electrolysis time. *J. Environ. Chem. Eng.* **2020**, *8*, 104368. [CrossRef]
16. Dura, A.; Breslin, C.B. Electrocoagulation using stainless steel anodes: Simultaneous removal of phosphates, Orange II and zinc ions. *J. Hazard. Mater.* **2019**, *374*, 152–158. [CrossRef] [PubMed]
17. Greenberg, A.; Eaton, A.; Clesceri, L. *Standard Methods for the Examination of Water and Wastewater*, 23rd ed.; American Public Health Association (APHA): Washington, DC, USA, 2017.
18. Atmaca, E. Treatment of landfill leachate by using electro-Fenton method. *J. Hazard. Mater.* **2009**, *163*, 109–114. [CrossRef]
19. Vale-Júnior, E.; Silva, D.R.; Fajardo, A.S.; Martínez-Huitle, C.A. Treatment of an azo dye effluent by peroxi-coagulation and its comparison to traditional electrochemical advanced processes. *Chemosphere* **2018**, *204*, 548–555. [CrossRef]
20. *ISO 18763:2016*; Soil Quality—Determination of the Toxic Effects of Pollutants on Germination and Early Growth of Higher Plants; Edition 1. International Organization for Standardization: Geneva, Switzerland, 2016.
21. Rodrigues, A.; Brito, A.; Janknecht, P.; Proença, M.F.; Nogueira, R. Quantification of humic acids in surface water: Effects of divalent cations, pH, and filtration. *J. Environ. Monit.* **2009**, *11*, 377–382. [CrossRef]
22. Gómez, M.; Corona, F.; Hidalgo, M.D. Variations in the properties of leachate according to landfill age. *Desalination Water Treat.* **2019**, *159*, 24–31. [CrossRef]
23. Fajardo, A.; Rodrigues, R.F.; Martins, R.C.; Castro, L.M.; Quinta Ferreira, R.M. Phenolic wastewaters treatment by electrocoagulation process using Zn anode. *Chem. Eng. J.* **2015**, *275*, 331–341. [CrossRef]
24. Beverskog, B.; Puigdomenech, I. Revised pourbaix diagrams for iron at 25–300 °C. *Corros. Sci.* **1996**, *12*, 2121–2135. [CrossRef]

25. Asaithambi, P.; Beyene, D.; Aziz, A.; Alemayehu, E. Removal of pollutants with determination of power consumption from landfill leachate wastewater using an electrocoagulation process: Optimization using response surface methodology (RSM). *Appl. Water Sci.* **2018**, *8*, 69. [CrossRef]
26. Deng, Y.; Chen, N.; Hu, W.; Wang, H.; Kuang, P.; Chen, F.; Feng, C. Treatment of old landfill leachate by persulfate enhanced electro-coagulation system: Improving organic matters removal precipitates settling performance. *Chem. Eng. J.* **2021**, *424*, 130262. [CrossRef]
27. Turro, E.; Giannis, A.; Cossu, R.; Gidarakos, E.; Mantzavinos, D.; Katsaounis, A. Electrochemical oxidation of stabilized landfill leachate on DSA electrodes. *J. Hazard. Mater.* **2011**, *190*, 460–465. [CrossRef]
28. Keyikoglu, R.; Can, O.T.; Aygun, A.; Tek, A. Comparison of the effects of various supporting electrolytes on the treatment of a dye solution by electrocoagulation process. *Colloid Interface Sci. Commun.* **2019**, *33*, 100210. [CrossRef]
29. Beiramzadeh, Z.; Baqersad, M.; Aghababaei, M. Application of the response surface methodology (RSM) in heavy metal removal from real power plant wastewater using electrocoagulation. *Eur. J. Environ. Civ. Eng.* **2022**, *26*, 1–20. [CrossRef]
30. Angarnokolaei, M.A.; Ganjidoust, H.; Ayati, B. Optimization of parameters of electrocoagulation/flotation process for removal of Acid Red 14 with mesh stainless steel electrodes. *J. Water Reuse Desalination* **2018**, *8*, 278–292. [CrossRef]
31. Abdullah, A.Z.; Amanullah, H.; Abdurahman, M.H.; Basir, N.I. Treatment of Stabilized Sanitary Landfill Leachate Using Electrocoagulation Process Equipped with Fe, Al, and Zn Electrodes and Assisted by Cationic Polyacrylamide Coagulant Aid. *Arab. J. Sci. Eng.* **2023**, *48*, 8495–8506. [CrossRef]
32. Ahmed, Z.; Yusoff, M.S.; Kamal, N.H.M.; Aziz, H.A. Humic acid recovery from stabilized leachate: Characterization and interference with chemical oxygen demand–colour removal. *Waste Manag. Res.* **2023**, *41*, 1584–1593. [CrossRef]
33. Lee, H.; Coulon, F.; Wagland, S.T. The influence of humic acid on metal(loid)s leaching in landfill leachate for enhancing landfill mining. *Sci. Total Environ.* **2023**, *896*, 165250. [CrossRef] [PubMed]
34. Bakry, S.A.; Matta, M.E.; Noureldin, A.M.; Zaher, K. Performance evaluation of electrocoagulation process for removal of heavy metals from wastewater using aluminum electrodes under variable operating conditions. *Desalination Water Treat.* **2024**, *318*, 100396. [CrossRef]